


Exciton-Scattering-Induced Dephasing in Two-Dimensional Semiconductors

Florian Katsch¹,* Malte Selig¹, and Andreas Knorr

Institut für Theoretische Physik, Nichtlineare Optik und Quantenelektronik, Technische Universität Berlin, 10623 Berlin, Germany

 (Received 16 October 2019; revised manuscript received 25 January 2020; accepted 1 June 2020; published 24 June 2020)

Enhanced Coulomb interactions in monolayer transition metal dichalcogenides cause tightly bound electron-hole pairs (excitons) that dominate their linear and nonlinear optical response. The latter includes bleaching, energy renormalizations, and higher-order Coulomb correlation effects like biexcitons and excitation-induced dephasing. While the first three are extensively studied, no theoretical footing for excitation-induced dephasing in exciton-dominated semiconductors is available so far. In this Letter, we present microscopic calculations based on excitonic Heisenberg equations of motion and identify the coupling of optically pumped excitons to exciton-exciton scattering continua as the leading mechanism responsible for an optical-power-dependent linewidth broadening (excitation-induced dephasing) and sideband formation. Performing time-, momentum-, and energy-resolved simulations, we quantitatively evaluate the exciton-induced dephasing for the most common monolayer transition metal dichalcogenides and find an excellent agreement with recent experiments.

DOI: [10.1103/PhysRevLett.124.257402](https://doi.org/10.1103/PhysRevLett.124.257402)

The widely investigated nonlinear optical response performed on III–V quantum wells involves bleaching and energy renormalizations of the optical transitions, as well as nonperturbative electronic correlation effects like biexciton formation and a spectral linewidth increase with rising excitation density. The latter, often referred to as excitation-induced dephasing (EID) [1–11], originates from the simultaneous optical excitation of excitons and incoherent electron-hole plasma interacting via frequency-dependent screened Coulomb interactions with nonzero imaginary part as demonstrated within a kinetic Markovian Boltzmann-like scattering theory [4].

However, recent advances in growth technology enabled the fabrication of purely two-dimensional semiconductors [12] including monolayers of transition metal dichalcogenides (TMDCs) [13,14]. The reduced dimensionality and strong Coulomb interactions enabled the investigation of nearly pure excitonic systems with tightly bound electron-hole pairs (excitons) separated by hundreds of meV from the free particle band gap [15,16]. Hence, intense many-body effects make atomically thin TMDCs ideal candidates for studying a completely new type of EID originating from exciton-exciton scattering in the absence of free electron-hole plasma [17–22]. Whereas an enhancement of the EID in monolayer TMDCs by one order of magnitude compared to conventional semiconductor quantum wells was experimentally demonstrated [17], a profound theoretical understanding of underlying mechanisms is still missing.

In this Letter, we provide a microscopic description of EID of excitons in two-dimensional semiconductors. Our

approach is based on the excitonic Heisenberg equation of motion formalism [23,24], including the Coulomb coupling of optically pumped excitons to (i) other excitons, (ii) biexcitons [25–34] detectable below the energetically lowest excitons (binding energy $2\epsilon_x - \epsilon_{xx}$) [35–38], and (iii) unbound solutions of the two-electron and two-hole Schrödinger equation, cf. Fig. 1. The latter describe continuous Coulomb correlated exciton-exciton scattering states setting in at twice the exciton energy $2\epsilon_x$ [39–50] and provide new scattering channels for optically addressable excitons. Based on time-, momentum-, and energy-resolved simulations, we quantitatively identify the coupling of excitons to exciton-exciton scattering continua as the leading mechanism for the excitation-power-dependent linewidth broadening. We calculate a linear increase of the exciton linewidth with rising excitation power for the most common TMDCs and find an excellent agreement with available experiments [17,20,22]. Additionally, we report excitation-power-dependent asymmetric line shapes with sidebands on the high-energy sides of exciton resonances, as expected from the fluctuation-dissipation theorem, originating from the non-Markovian interaction of excitons with exciton-exciton scattering continua.

Excitonic description.—Bound electron-hole pairs are described by first solving the Wannier equation, which provides the exciton energies $\epsilon_{x,\lambda}$ as well as wave functions $\varphi_{\lambda,q}$ [51], and subsequently calculating the dynamics of the excitonic interband transitions $P_\lambda(t)$ [24]. λ as a compound index incorporates the exciton state, the high-symmetry point, and the spins of involved electrons and holes. The Heisenberg equation of motion for optically addressable

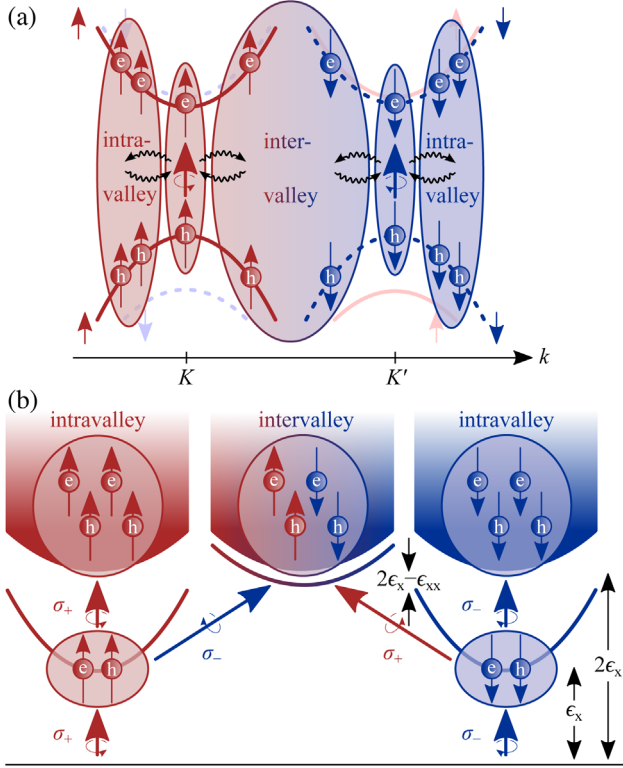


FIG. 1. Excitonic correlations in monolayer TMDCs. (a) $\sigma_{+(-)}$ polarized light introduces bound electron-hole pairs (excitons) near the corner $K^{(l)}$ of the hexagonal Brillouin zone. In the nonlinear regime, optically addressable excitons interact via Coulomb interactions with two-electron and two-hole Coulomb intravalley and intervalley correlations. (b) Optically addressable excitons with energy ϵ_x couple to intravalley exciton-exciton scattering continua setting in at $2\epsilon_x$ excited by σ_+ or σ_- polarized light, as well as intervalley biexcitons separated by $2\epsilon_x - \epsilon_{xx}$ from the associated intervalley exciton-exciton scattering states addressed by the simultaneous excitation with σ_+ and σ_- polarized light.

excitonic transitions P_{λ} reads (cf. Supplemental Material Sec. 1 [52])

$$\begin{aligned}
 & (\hbar\partial_t + \gamma_0 - i\epsilon_{x,\lambda_1})P_{\lambda_1} \\
 &= -id_{\lambda_1}E_{\sigma_{\pm}}(t) + i\sum_{\lambda_2,\lambda_3}\hat{d}_{\lambda_1,\lambda_2,\lambda_3}E_{\sigma_{\pm}}(t)P_{\lambda_2}P_{\lambda_3}^* \\
 &+ i\sum_{\lambda_2}V_{\lambda_1,\lambda_2}P_{\lambda_2} + i\sum_{\lambda_2,\lambda_3,\lambda_4}\hat{V}_{\lambda_1,\lambda_2,\lambda_3,\lambda_4}P_{\lambda_2}P_{\lambda_3}P_{\lambda_4}^* \\
 &+ i\sum_{\lambda_2,\eta}W_{\lambda_1,\lambda_2,\eta}B_{\eta}P_{\lambda_2}^*. \quad (1)
 \end{aligned}$$

Equation (1) describes optical oscillations (energy ϵ_{x,λ_1}) damped by the microscopically calculated phonon-mediated dephasing rate γ_0 [92] (cf. Supplemental Material Sec. 2 [52]). $\sigma_{+(-)}$ circularly polarized light $E_{\sigma_{+(-)}}(t)$ drives P_{λ_1} according to the optical selection rules [93] incorporated in the excitonic dipole matrix element d_{λ_1}

(first term in the second line). Self-consistently solving the TMDC Bloch equations and Maxwell's equations determines the radiative dephasing [94]. Additionally, the exciton-light interaction involves Pauli blocking (second term in the second line). Coulomb scattering comprises linear and nonlinear Hartree-Fock interactions (third line) and the coupling of excitons to two-electron and two-hole Coulomb correlations B_{η} (fourth line) [95]. η comprises the high-symmetry points and spins of the two electrons and two holes.

Solving the *intravalley* two-electron and two-hole Schrödinger equation for two electrons and two holes at the K point accesses intravalley exciton-exciton scattering continua energetically above the exciton energy, cf. Fig. 1(b). In addition to the intervalley exciton-exciton scattering continua, the *intervalley* four-particle eigenvalue problem with one electron and hole near the K point and one electron and hole near the K' point results in bound intervalley biexcitons. Biexcitons are observed energetically below the exciton resonance due to the attractive interaction of two virtual excitons with opposite spins near distinguished high-symmetry points. The Heisenberg equations of motion for biexcitons and exciton-exciton scattering states B_{η} describe damped (γ_{xx}) oscillations (energy $\epsilon_{xx,\eta}$) self-consistently coupling to two excitons $P_{\lambda_1}P_{\lambda_2}$ mediated by Coulomb interactions ($\hat{W}_{\eta,\lambda_1,\lambda_2}$) [96],

$$(\hbar\partial_t + \gamma_{xx} + i\epsilon_{xx,\eta})B_{\eta} = i\sum_{\lambda_1,\lambda_2}\hat{W}_{\eta,\lambda_1,\lambda_2}P_{\lambda_1}P_{\lambda_2}. \quad (2)$$

Results.—Self-consistently evaluating the coupled exciton, biexciton, and exciton-exciton scattering continua dynamics, Eqs. (1) and (2), together with Maxwell's equations [94] in a nonperturbative way accesses [97] the nonlinear frequency-dependent absorption $\alpha(\omega) = 1 - T(\omega) - R(\omega)$ defined with respect to the transmission $T(\omega)$ and reflection $R(\omega)$ [51]. Figures 2(a) and 2(b) shows the absorption of the energetically lowest optically addressable exciton for resonant excitation of WSe₂ on a SiO₂ substrate at 10 K with [Fig. 2(a)] circularly or [Fig. 2(b)] linearly polarized, 40 fs pulses. With increasing pump fluence of the exciting light field, (i) the maximum of the absorption bleaches, (ii) the absorption peak shifts toward higher energies, (iii) the absorption broadens, and (iv) for linearly polarized light a biexciton resonance appears. We identify the following mechanisms for the different observations: (i) The decreasing nonlinear absorption for intensified pump fluences has two reasons—first, Pauli blocking quenching the light-matter interaction, and second, exciton-exciton scattering redistributing the oscillator strength. However, in the weakly nonlinear regime, the latter dominates and Pauli blocking is minor [98], (ii) The excitation-induced shift of the excitonic resonance energy originates from Coulomb-induced band gap renormalization and mean field contributions. Whereas Hartree-Fock

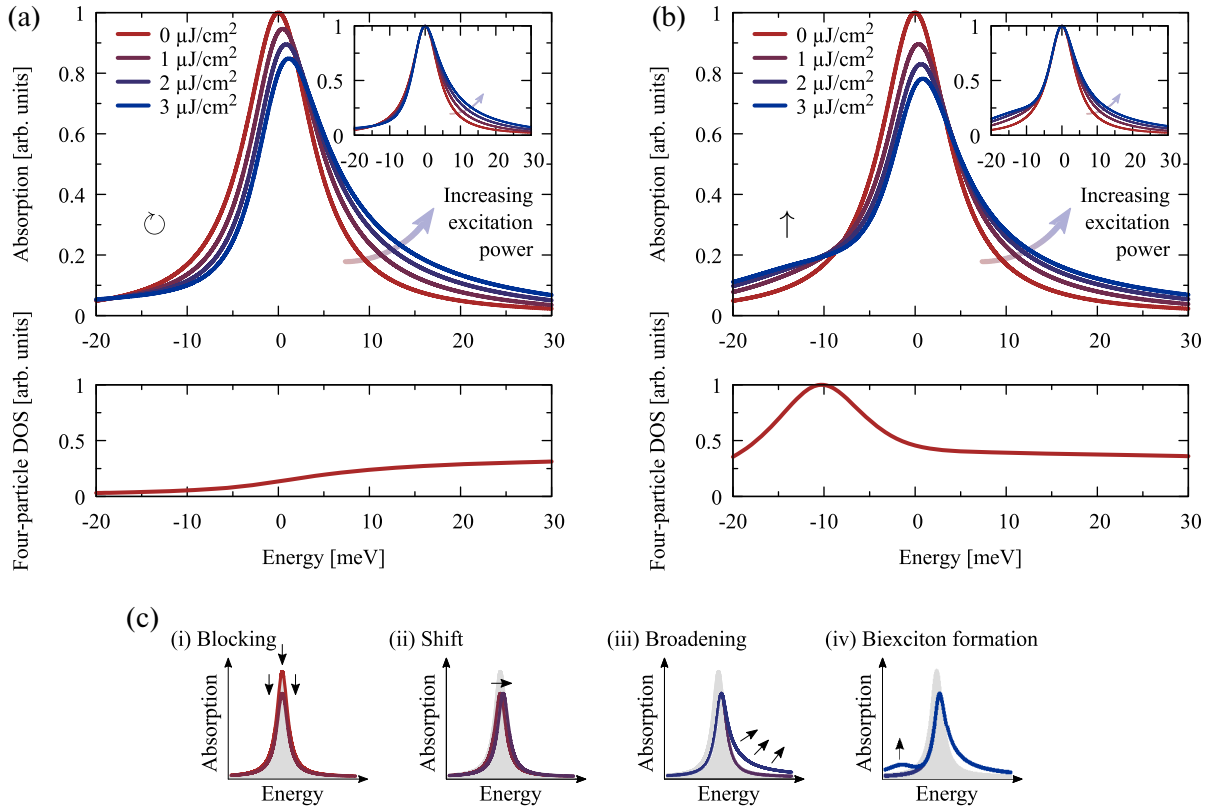


FIG. 2. Nonlinear absorption of WSe₂. (a),(b) Depicted is the nonlinear absorption spectrum of monolayer WSe₂ on a SiO₂ substrate at 10 K for different pump fluences. The energetically lowest optically addressable exciton is resonantly excited by (a) circularly (⊙) or (b) linearly (↑) polarized, 40 fs pulses. (Insets) Normalized and shifted absorption revealing non-Markovian sidebands on the high-energy sides of the exciton resonances, which become more pronounced for higher excitation densities. The four-particle (two-electron and two-hole) densities of states (DOS) for circularly and linearly polarized excitation are plotted below. (c) Illustrated are the four effects observed in the microscopically calculated nonlinear absorption, namely, (i) a blocking of the absorption, (ii) a shift of the resonance energy, (iii) a line broadening originating from a sideband formation on the high-energy side of the exciton resonance, and (iv) the formation of biexcitons for linearly polarized excitation. The shaded area represents the absorption for negligibly small excitation strength.

effects [second to last contribution to Eq. (1)] induce a blueshift, the exciton-exciton scattering continua [last contribution to Eq. (1)] cause a smaller redshift. The interplay of both results in an effective blueshift [99] as observed in coherent pump-probe experiments [102–106], and (iii) The absorption spectra indicate a line broadening [cf. insets in Figs. 2(a) and 2(b)], associated with the formation of a pronounced shoulder on the high-energy side of the exciton resonance. This nonlinear effect exclusively arises from the Coulomb coupling among excitons, biexcitons, and exciton-exciton scattering states. To analyze the dominating effects for the broadening, the four-particle density of states, defined as the imaginary part of the corresponding two-electron and two-hole scattering matrix in the Supplemental Material Sec. 2 [52], is plotted below the absorption spectra in Figs. 2(a) and 2(b). The full four-particle density of states shows the exciton-exciton scattering continua above the exciton energy and an additional biexciton resonance below the exciton for linearly polarized excitation. This result clearly shows that

nonlinear Coulomb scattering redistributes the oscillator strength and leads to pronounced shoulders on the high-energy side of the exciton resonances. The effect resembles the non-Markovian coupling of excitons to the phonon continuum, which also causes a shoulder on the high-energy side accompanied by a polaron redshift [107–109]. However, whereas phonon sidebands disappear in the low temperature limit, the asymmetric line shape due to exciton-exciton interactions remains. Thus, changing the temperature at elevated excitation power allows to distinguish both effects in optical experiments.

(iv) For excitation with a linearly polarized pulse, the four-particle density of states exhibits a biexciton, resulting in a resonance energetically below the exciton in Fig. 2(b).

Analytical approach.—To provide an experimentally accessible evaluation of nonlinear line broadening effects in the coherent limit, we analytically extract the EID hereinafter. Applying a second-order Born-Markov approximation to eliminate the exciton-exciton scattering continua in Eq. (1) accesses the total linewidth of the

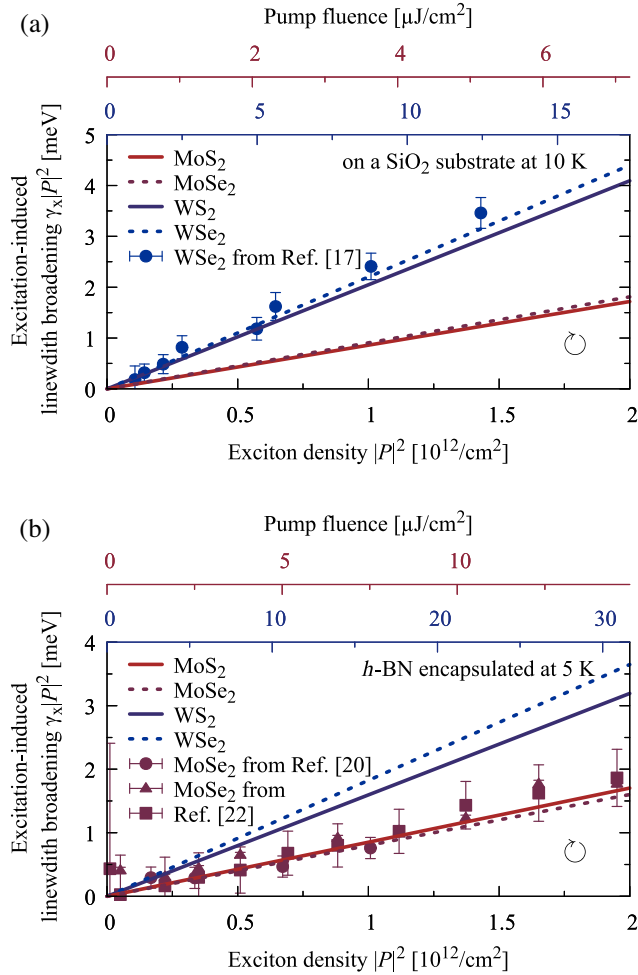


FIG. 3. Excitation-induced linewidth broadening. (a) Shown is the linearly increasing excitation-induced linewidth broadening $\gamma_x |P|^2$ depending on the exciton density $|P|^2$ for MoS₂, MoSe₂, WS₂, and WSe₂ on SiO₂ substrates at 10 K for circularly (\odot) polarized excitation. The pump fluence-dependent linewidth increases are extracted from the absorption spectra obtained from numerically solving Eq. (1) for 40 fs circularly polarized pulses. The dependence from the material absorption requires different axes roughly describing molybdenum- (upper, red) and tungsten-based (lower, blue) TMDCs. (b) Same as in (a) but for TMDCs encapsulated in *h*-BN at 5 K. The experimental data for WSe₂ and MoSe₂ adopted from Refs. [17,20,22] are divided by 1.1 and 0.3, respectively, to account for our calculations showing a 1.1 times larger or 0.3 times smaller excitation-induced linewidth increase measured in transmission and reflection compared to $\gamma_x |P|^2$ (cf. Supplemental Material Sec. 4).

energetically lowest exciton $P = P_{1s}$ in the K valley, which linearly increases with rising coherent exciton density $|P|^2$,

$$[\hbar\partial_t + \gamma_0 - i\hat{e}_x + (\gamma_x - iW_x)|P|^2]P = -iE_{\sigma_+}(d - \hat{d}|P|^2). \quad (3)$$

For the derivation, associated matrix elements, and comparison to the full numerical approach, see Supplemental Material Sec. 3 [52]. Contrary to conventional III-V

semiconductors, the EID in exciton-dominated materials is determined by coherent exciton densities instead of incoherent electron-hole densities [3–5]. Incoherent excitonic densities contribute only in the long time limit where exciton-phonon scattering dominates [110–114]. Therefore, in the investigated case of (near) resonant excitation, EID expressed by γ_x is determined by the exciton-exciton scattering continua solely.

To show the impact of our calculations, we analyze recent optical wave-mixing experiments [17,20,22]: Fig. 3(a) shows the microscopically calculated linear dependence between excitation-induced linewidth broadening $\gamma_x |P|^2$ and exciton density assuming circularly polarized optical excitation for monolayer MoS₂, MoSe₂, WS₂, and WSe₂ on SiO₂ substrates at 10 K along with experimental data from Ref. [17]. WSe₂ exhibits the largest slope, closely followed by WS₂. For a direct experiment-theory comparison, the experimental detection geometry (transmission or reflection) has to be taken into account to compare the measured values to the calculated nonlinear susceptibility (cf. Supplemental Material Sec. 4). For the transmission geometry studied in Ref. [17], we find a 1.1 times larger EID compared to the EID γ_x of the nonlinear susceptibility, which requires one to divide the experimental slope by 1.1. Our microscopically calculated EID for the nonlinear susceptibility $\gamma_x = 2.2 \times 10^{-12}$ meV cm² for WSe₂ is in very good agreement with the corrected measured value of 2.5×10^{-12} meV cm² [17]. Since molybdenum-based TMDCs exhibit smaller conduction and valence band curvatures near the $K^{(l)}$ point compared with tungsten-based TMDCs [115], the EID for MoS₂ and MoSe₂ is about a factor of 2 smaller.

Figure 3(b) depicts the excitation-induced linewidth broadening for TMDCs encapsulated in hexagonal boron nitride (*h*-BN) [116] at 5 K. Here, the enhanced screening compared with SiO₂ substrates yields smaller EID. Our calculated EID $\gamma_x = 0.8 \times 10^{-12}$ meV cm² for MoSe₂ is in excellent agreement with recent experiments, which measured a slope of 0.7×10^{-12} [20] and 0.9×10^{-12} meV cm² [22]. To take the reflection geometry into account, where we predict a 0.3 times smaller EID compared to the nonlinear susceptibility γ_x , the experimental values had to be divided by 0.3 to compare them to our calculated values for the nonlinear susceptibility (cf. Supplemental Material Sec. 4). Assuming identical excitation conditions, we find that the largest values for the excitation-induced linewidth broadening of a material can be measured in absorption and the second largest values in transmission (both larger than γ_x). The smallest excitation-induced linewidth broadening is recorded in reflection (smaller than γ_x).

Conclusion.—We identified the coupling of excitons to exciton-exciton scattering continua as the dominating mechanism for EID. The frequency-dependent linewidth broadening and shifts of the exciton resonance cause strong deviations from the symmetric Lorentzian line shape. Our

microscopical calculations are in good agreement with, so far, poorly understood experimental observations. We expect that our theoretical footing for EID is widely applicable to inorganic and organic semiconductors with tightly bound excitons, indicating strong Coulomb interactions and pronounced many-body effects for nonlinear excitation below the Mott transition, or other bosonic gases in condensed matter physics [117]. Possible candidates are not only other exciton-dominated two-dimensional structures, such as black phosphorus [118–122] or transition metal trichalcogenides [123,124], but also, for instance, thin CdSe [125] or perovskite nanoplatelets [126,127], and organic as well as hybrid organic-inorganic structures [128–130]. We believe that our Letter will trigger calculations in other material systems as our description is applicable once the excitonic eigenvalue problem is solved.

We thank Dominik Christiansen (TU Berlin) as well as Robert Schmidt and Rudolf Bratschitsch (WWU Münster) for stimulating discussions. We are particularly grateful to Galan Moody (UC Santa Barbara), Elaine Li (UT Austin), Eric Martin and Steven Cundiff (University of Michigan), Jacek Kasprzak (CNRS Grenoble) and all involved co-workers for allowing us to use their experimental data. We gratefully acknowledge support from the Deutsche Forschungsgemeinschaft via the Projects No. 420760124 (KN 427/11-1, F. K., A. K.) as well as No. 182087777—SFB 951 (B12, M. S., A. K.). We also acknowledge the support of the European Unions Horizon 2020 research and innovation program under Grant Agreement No. 734690 (SONAR, A. K.). F. K. thanks the Berlin School of Optical Sciences and Quantum Technology.

*fkatsch@itp.tu-berlin.de

- [1] L. Schultheis, J. Kuhl, A. Honold, and C. W. Tu, *Phys. Rev. Lett.* **57**, 1635 (1986).
- [2] A. Honold, L. Schultheis, J. Kuhl, and C. W. Tu, *Phys. Rev. B* **40**, 6442 (1989).
- [3] H. Wang, K. Ferrio, D. G. Steel, Y. Z. Hu, R. Binder, and S. W. Koch, *Phys. Rev. Lett.* **71**, 1261 (1993).
- [4] H. Wang, K. B. Ferrio, D. G. Steel, P. R. Berman, Y. Z. Hu, R. Binder, and S. W. Koch, *Phys. Rev. A* **49**, R1551 (1994).
- [5] Y. Z. Hu, R. Binder, S. W. Koch, S. T. Cundiff, H. Wang, and D. G. Steel, *Phys. Rev. B* **49**, 14382 (1994).
- [6] T. Rappen, U.-G. Peter, M. Wegener, and W. Schäfer, *Phys. Rev. B* **49**, 10774 (1994).
- [7] H. P. Wagner, A. Schätz, R. Maier, W. Langbein, and J. M. Hvam, *Phys. Rev. B* **56**, 12581 (1997).
- [8] H. P. Wagner, A. Schätz, W. Langbein, J. M. Hvam, and A. L. Smirl, *Phys. Rev. B* **60**, 4454 (1999).
- [9] X. Li, T. Zhang, C. N. Borca, and S. T. Cundiff, *Phys. Rev. Lett.* **96**, 057406 (2006).
- [10] G. Moody, M. E. Siemens, A. D. Bristow, X. Dai, D. Karaickaj, A. S. Bracker, D. Gammon, and S. T. Cundiff, *Phys. Rev. B* **83**, 115324 (2011).
- [11] G. Nardin, G. Moody, R. Singh, T. M. Autry, H. Li, F. Morier-Genoud, and S. T. Cundiff, *Phys. Rev. Lett.* **112**, 046402 (2014).
- [12] K. S. Novoselov, D. Jiang, F. Schedin, T. Booth, V. Khotkevich, S. Morozov, and A. K. Geim, *Proc. Natl. Acad. Sci. U.S.A.* **102**, 10451 (2005).
- [13] K. F. Mak, C. Lee, J. Hone, J. Shan, and T. F. Heinz, *Phys. Rev. Lett.* **105**, 136805 (2010).
- [14] A. Splendiani, L. Sun, Y. Zhang, T. Li, J. Kim, C.-Y. Chim, G. Galli, and F. Wang, *Nano Lett.* **10**, 1271 (2010).
- [15] T. C. Berkelbach, M. S. Hybertsen, and D. R. Reichman, *Phys. Rev. B* **88**, 045318 (2013).
- [16] A. Chernikov, T. C. Berkelbach, H. M. Hill, A. Rigosi, Y. Li, O. B. Aslan, D. R. Reichman, M. S. Hybertsen, and T. F. Heinz, *Phys. Rev. Lett.* **113**, 076802 (2014).
- [17] G. Moody, C. K. Dass, K. Hao, C.-H. Chen, L.-J. Li, A. Singh, K. Tran, G. Clark, X. Xu, G. Berghäuser *et al.*, *Nat. Commun.* **6**, 8315 (2015).
- [18] P. Dey, J. Paul, Z. Wang, C. E. Stevens, C. Liu, A. H. Romero, J. Shan, D. J. Hilton, and D. Karaickaj, *Phys. Rev. Lett.* **116**, 127402 (2016).
- [19] F. Mahmood, Z. Alpichshev, Y.-H. Lee, J. Kong, and N. Gedik, *Nano Lett.* **18**, 223 (2017).
- [20] E. W. Martin, J. Horng, H. G. Ruth, E. Paik, M.-H. Wentzel, H. Deng, and S. T. Cundiff, [arXiv:1810.09834](https://arxiv.org/abs/1810.09834).
- [21] T. Jakubczyk, G. Nayak, L. Scarpelli, W.-L. Liu, S. Dubey, N. Bendiab, L. Marty, T. Taniguchi, K. Watanabe, F. Masia *et al.*, *ACS Nano* **13**, 3500 (2019).
- [22] C. Boule, D. Vaclavkova, M. Bartos, K. Nogajewski, L. Zdražil, T. Taniguchi, K. Watanabe, M. Potemski, and J. Kasprzak, *Phys. Rev. Mater.* **4**, 034001 (2020).
- [23] A. L. Ivanov and H. Haug, *Phys. Rev. B* **48**, 1490 (1993).
- [24] F. Katsch, M. Selig, A. Carmele, and A. Knorr, *Phys. Status Solidi (b)* **255**, 1800185 (2018).
- [25] I. Kylänpää and H.-P. Komsa, *Phys. Rev. B* **92**, 205418 (2015).
- [26] M. Z. Mayers, T. C. Berkelbach, M. S. Hybertsen, and D. R. Reichman, *Phys. Rev. B* **92**, 161404(R) (2015).
- [27] D. K. Zhang, D. W. Kidd, and K. Varga, *Nano Lett.* **15**, 7002 (2015).
- [28] D. W. Kidd, D. K. Zhang, and K. Varga, *Phys. Rev. B* **93**, 125423 (2016).
- [29] E. Mostaani, M. Szyniszewski, C. H. Price, R. Maezono, M. Danovich, R. J. Hunt, N. D. Drummond, and V. I. Fal’ko, *Phys. Rev. B* **96**, 075431 (2017).
- [30] R. Y. Kezerashvili and S. M. Tsiklauri, *Few-Body Syst.* **58**, 18 (2017).
- [31] M. Szyniszewski, E. Mostaani, N. D. Drummond, and V. I. Fal’ko, *Phys. Rev. B* **95**, 081301(R) (2017).
- [32] M. Van der Donck, M. Zarenia, and F. M. Peeters, *Phys. Rev. B* **97**, 195408 (2018).
- [33] A. Steinhoff, M. Florian, A. Singh, K. Tran, M. Kolarczik, S. Helmrich, A. W. Achtstein, U. Woggon, N. Owschimikow, F. Jahnke *et al.*, *Nat. Phys.* **14**, 1199 (2018).
- [34] S. C. Kuhn and M. Richter, *Phys. Rev. B* **99**, 241301(R) (2019).
- [35] E. J. Sie, A. J. Frenzel, Y.-H. Lee, J. Kong, and N. Gedik, *Phys. Rev. B* **92**, 125417 (2015).

- [36] S. H. Aleithan, M. Y. Livshits, S. Khadka, J. J. Rack, M. E. Kordesch, and E. Stinaff, *Phys. Rev. B* **94**, 035445 (2016).
- [37] E. J. Sie, C. H. Lui, Y.-H. Lee, J. Kong, and N. Gedik, *Nano Lett.* **16**, 7421 (2016).
- [38] K. Hao, J. F. Specht, P. Nagler, L. Xu, K. Tran, A. Singh, C. K. Dass, C. Schüller, T. Korn, M. Richter *et al.*, *Nat. Commun.* **8**, 15552 (2017).
- [39] V. Axt, K. Victor, and T. Kuhn, *Phys. Status Solidi (b)* **206**, 189 (1998).
- [40] G. Bartels, A. Stahl, V. M. Axt, B. Haase, U. Neukirch, and J. Gutowski, *Phys. Rev. Lett.* **81**, 5880 (1998).
- [41] N. H. Kwong, R. Takayama, I. Romyantsev, M. Kuwata-Gonokami, and R. Binder, *Phys. Rev. B* **64**, 045316 (2001).
- [42] N.-H. Kwong, R. Takayama, I. Romyantsev, M. Kuwata-Gonokami, and R. Binder, *Phys. Rev. Lett.* **87**, 027402 (2001).
- [43] R. Takayama, N. Kwong, I. Romyantsev, M. Kuwata-Gonokami, and R. Binder, *Eur. Phys. J. B* **25**, 445 (2002).
- [44] T. Voss, H. G. Breunig, I. Rückmann, J. Gutowski, V. M. Axt, and T. Kuhn, *Phys. Rev. B* **66**, 155301 (2002).
- [45] S. Schumacher, G. Czycholl, F. Jahnke, I. Kudyk, L. Wischmeier, I. Rückmann, T. Voss, J. Gutowski, A. Gust, and D. Hommel, *Phys. Rev. B* **72**, 081308(R) (2005).
- [46] S. Schumacher, G. Czycholl, and F. Jahnke, *Phys. Rev. B* **73**, 035318 (2006).
- [47] T. Voss, I. Rückmann, J. Gutowski, V. M. Axt, and T. Kuhn, *Phys. Rev. B* **73**, 115311 (2006).
- [48] S. Schumacher, N.-H. Kwong, and R. Binder, *Phys. Rev. B* **76**, 245324 (2007).
- [49] W. Schäfer and M. Wegener, *Semiconductor Optics and Transport Phenomena* (Springer Science + Business Media, New York, 2013).
- [50] F. Katsch, M. Selig, and A. Knorr, *2D Mater.* **7**, 015021 (2020).
- [51] M. Kira and S. W. Koch, *Prog. Quantum Electron.* **30**, 155 (2006).
- [52] See Supplemental Material at <http://link.aps.org/supplemental/10.1103/PhysRevLett.124.257402> for details on the theoretical description, which includes Refs. [53–91].
- [53] D. Y. Qiu, T. Cao, and S. G. Louie, *Phys. Rev. Lett.* **115**, 176801 (2015).
- [54] Q. H. Wang, K. Kalantar-Zadeh, A. Kis, J. N. Coleman, and M. S. Strano, *Nat. Nanotechnol.* **7**, 699 (2012).
- [55] M. Chhowalla, H. S. Shin, G. Eda, L.-J. Li, K. P. Loh, and H. Zhang, *Nat. Chem.* **5**, 263 (2013).
- [56] F. A. Rasmussen and K. S. Thygesen, *J. Phys. Chem. C* **119**, 13169 (2015).
- [57] M. L. Trolle, T. G. Pedersen, and V. Vénier, *Sci. Rep.* **7**, 39844 (2017).
- [58] S. Latini, T. Olsen, and K. S. Thygesen, *Phys. Rev. B* **92**, 245123 (2015).
- [59] K. Andersen, S. Latini, and K. S. Thygesen, *Nano Lett.* **15**, 4616 (2015).
- [60] D. Y. Qiu, F. H. da Jornada, and S. G. Louie, *Phys. Rev. B* **93**, 235435 (2016).
- [61] A. Steinhoff, M. Florian, M. Rösner, G. Schönhoff, T. O. Wehling, and F. Jahnke, *Nat. Commun.* **8**, 1166 (2017).
- [62] S. C. Kuhn and M. Richter, *Phys. Rev. B* **101**, 075302 (2020).
- [63] H. Haug and S. W. Koch, *Quantum Theory of the Optical and Electronic Properties of Semiconductors* (World Scientific, Singapore, 2009).
- [64] A. Ramasubramaniam, *Phys. Rev. B* **86**, 115409 (2012).
- [65] T. Cheiwchanchamnangij and W. R. Lambrecht, *Phys. Rev. B* **85**, 205302 (2012).
- [66] L. Guo, M. Wu, T. Cao, D. M. Monahan, Y.-H. Lee, S. G. Louie, and G. R. Fleming, *Nat. Phys.* **15**, 228 (2019).
- [67] T. Deilmann and K. S. Thygesen, *2D Mater.* **6**, 035003 (2019).
- [68] H. Yu, G.-B. Liu, P. Gong, X. Xu, and W. Yao, *Nat. Commun.* **5**, 3876 (2014).
- [69] M. M. Glazov, T. Amand, X. Marie, D. Lagarde, L. Bouet, and B. Urbaszek, *Phys. Rev. B* **89**, 201302(R) (2014).
- [70] T. Stroucken, A. Knorr, P. Thomas, and S. W. Koch, *Phys. Rev. B* **53**, 2026 (1996).
- [71] G. Cappellini, R. Del Sole, L. Reining, and F. Bechstedt, *Phys. Rev. B* **47**, 9892 (1993).
- [72] A. Kumar and P. Ahluwalia, *Physica (Amsterdam)* **407B**, 4627 (2012).
- [73] A. Torche and G. Bester, *Phys. Rev. B* **100**, 201403(R) (2019).
- [74] Z. Lu, D. Rhodes, Z. Li, D. Van Tuan, Y. Jiang, J. Ludwig, Z. Jiang, Z. Lian, S. Shi, J. C. Hone *et al.*, *2D Mater.* **7**, 015017 (2020).
- [75] G. E. Pikus and G. L. Bir, *J. Exp. Theor. Phys.* **33**, 108 (1971).
- [76] G. E. Pikus and G. L. Bir, *J. Exp. Theor. Phys.* **35**, 174 (1972).
- [77] L. C. Andreani and F. Bassani, *Phys. Rev. B* **41**, 7536 (1990).
- [78] C. Ciuti, V. Savona, C. Piermarocchi, A. Quattropani, and P. Schwendimann, *Phys. Rev. B* **58**, 7926 (1998).
- [79] S. Brem, J. Zipfel, M. Selig, A. Raja, L. Waldecker, J. Ziegler, T. Taniguchi, K. Watanabe, A. Chernikov, and E. Malić, *Nanoscale* **11**, 12381 (2019).
- [80] X. Li, J. T. Mullen, Z. Jin, K. M. Borysenko, M. Buongiorno Nardelli, and K. W. Kim, *Phys. Rev. B* **87**, 115418(R) (2013).
- [81] Z. Jin, X. Li, J. T. Mullen, and K. W. Kim, *Phys. Rev. B* **90**, 045422 (2014).
- [82] J. Schilp, T. Kuhn, and G. Mahler, *Phys. Rev. B* **50**, 5435 (1994).
- [83] C. Zhang, H. Wang, W. Chan, C. Manolatou, and F. Rana, *Phys. Rev. B* **89**, 205436 (2014).
- [84] F. Cadiz, E. Courtade, C. Robert, G. Wang, Y. Shen, H. Cai, T. Taniguchi, K. Watanabe, H. Carrere, D. Lagarde *et al.*, *Phys. Rev. X* **7**, 021026 (2017).
- [85] Z. Khatibi, M. Feierabend, M. Selig, S. Brem, C. Linderäl, P. Erhart, and E. Malić, *2D Mater.* **6**, 015015 (2019).
- [86] G. Gupta and K. Majumdar, *Phys. Rev. B* **99**, 085412 (2019).
- [87] I. C. Gerber and X. Marie, *Phys. Rev. B* **98**, 245126 (2018).
- [88] H. H. Fang, B. Han, C. Robert, M. A. Semina, D. Lagarde, E. Courtade, T. Taniguchi, K. Watanabe, T. Amand, B. Urbaszek *et al.*, *Phys. Rev. Lett.* **123**, 067401 (2019).

- [89] A. Steinhoff, T. O. Wehling, and M. Rösner, *Phys. Rev. B* **98**, 045304 (2018).
- [90] A. Steinhoff, M. Florian, and F. Jahnke, *Phys. Rev. B* **101**, 045411 (2020).
- [91] E. Ridolfi, C. H. Lewenkopf, and V. M. Pereira, *Phys. Rev. B* **97**, 205409 (2018).
- [92] M. Selig, G. Berghäuser, A. Raja, P. Nagler, C. Schüller, T. F. Heinz, T. Korn, A. Chernikov, E. Malić, and A. Knorr, *Nat. Commun.* **7**, 13279 (2016).
- [93] D. Xiao, G.-B. Liu, W. Feng, X. Xu, and W. Yao, *Phys. Rev. Lett.* **108**, 196802 (2012).
- [94] A. Knorr, S. Hughes, T. Stroucken, and S. W. Koch, *Chem. Phys.* **210**, 27 (1996).
- [95] V. Axt and A. Stahl, *Z. Phys. B* **93**, 195 (1994).
- [96] As biexcitons and continuous exciton-exciton scattering states are Coulomb generated by two exciton transitions, a radiative part (as contributing to the exciton linewidth) does not occur in γ_{xx} linewidth, which in addition to a phonon-mediated part γ_0 also includes a radiative contribution.
- [97] B. Haase, U. Neukirch, J. Meinertz, J. Gutowski, V. M. Axt, G. Bartels, A. Stahl, J. Nürnberger, and W. Faschinger, *J. Cryst. Growth* **214–215**, 852 (2000).
- [98] R. Emmanuele, M. Sich, O. Kyriienko, V. Shahnazaryan, F. Withers, A. Catanzaro, P. Walker, F. Benimetskiy, M. Skolnick, A. Tartakovskii *et al.*, [arXiv:1910.14636](https://arxiv.org/abs/1910.14636).
- [99] Note that in the incoherent limit of a thermalized electron-hole plasma after well above band edge excitation, pronounced band gap shrinkage can lead to a redshift [100,101].
- [100] A. Steinhoff, M. Rosner, F. Jahnke, T. O. Wehling, and C. Gies, *Nano Lett.* **14**, 3743 (2014).
- [101] D. Erben, A. Steinhoff, C. Gies, G. Schönhoff, T. O. Wehling, and F. Jahnke, *Phys. Rev. B* **98**, 035434 (2018).
- [102] C. Mai, Y. G. Semenov, A. Barrette, Y. Yu, Z. Jin, L. Cao, K. W. Kim, and K. Gundogdu, *Phys. Rev. B* **90**, 041414(R) (2014).
- [103] E. J. Sie, J. W. McIver, Y.-H. Lee, L. Fu, J. Kong, and N. Gedik, *Nat. Mater.* **14**, 290 (2015).
- [104] Y.-T. Wang, C.-W. Luo, A. Yabushita, K.-H. Wu, T. Kobayashi, C.-H. Chen, and L.-J. Li, *Sci. Rep.* **5**, 8289 (2015).
- [105] E. J. Sie, C. H. Lui, Y.-H. Lee, L. Fu, J. Kong, and N. Gedik, *Science* **355**, 1066 (2017).
- [106] C.-K. Yong, J. Horng, Y. Shen, H. Cai, A. Wang, C.-S. Yang, C.-K. Lin, S. Zhao, K. Watanabe, T. Taniguchi *et al.*, *Nat. Phys.* **14**, 1092 (2018).
- [107] D. Christiansen, M. Selig, G. Berghäuser, R. Schmidt, I. Niehues, R. Schneider, A. Arora, S. M. de Vasconcellos, R. Bratschitsch, E. Malić *et al.*, *Phys. Rev. Lett.* **119**, 187402 (2017).
- [108] S. Shree, M. Semina, C. Robert, B. Han, T. Amand, A. Balocchi, M. Manca, E. Courtade, X. Marie, T. Taniguchi *et al.*, *Phys. Rev. B* **98**, 035302 (2018).
- [109] F. Lengers, T. Kuhn, and D. E. Reiter, *Phys. Rev. B* **101**, 155304 (2020).
- [110] R. Schmidt, G. Berghäuser, R. Schneider, M. Selig, P. Tonndorf, E. Malic, A. Knorr, S. M. de Vasconcellos, and R. Bratschitsch, *Nano Lett.* **16**, 2945 (2016).
- [111] M. Selig, G. Berghäuser, M. Richter, R. Bratschitsch, A. Knorr, and E. Malić, *2D Mater.* **5**, 035017 (2018).
- [112] M. Selig, F. Katsch, R. Schmidt, S. Michaelis de Vasconcellos, R. Bratschitsch, E. Malić, and A. Knorr, *Phys. Rev. Research* **1**, 022007(R) (2019).
- [113] D. Christiansen, M. Selig, E. Malić, R. Ernstorfer, and A. Knorr, *Phys. Rev. B* **100**, 205401 (2019).
- [114] M. Selig, F. Katsch, S. Brem, G. F. Mkrtchian, E. Malić, and A. Knorr, *Phys. Rev. Research* **2**, 023322 (2020).
- [115] A. Kormányos, G. Burkard, M. Gmitra, J. Fabian, V. Zólyomi, N. D. Drummond, and V. Fal'ko, *2D Mater.* **2**, 022001 (2015).
- [116] T. Taniguchi and K. Watanabe, *J. Cryst. Growth* **303**, 525 (2007).
- [117] K. Afrousheh, P. Bohlouli-Zanjani, D. Vagale, A. Mugford, M. Fedorov, and J. D. D. Martin, *Phys. Rev. Lett.* **93**, 233001 (2004).
- [118] H. Liu, A. T. Neal, Z. Zhu, Z. Luo, X. Xu, D. Tománek, and P. D. Ye, *ACS Nano* **8**, 4033 (2014).
- [119] V. Tran, R. Soklaski, Y. Liang, and L. Yang, *Phys. Rev. B* **89**, 235319 (2014).
- [120] L. Li, Y. Yu, G. J. Ye, Q. Ge, X. Ou, H. Wu, D. Feng, X. H. Chen, and Y. Zhang, *Nat. Nanotechnol.* **9**, 372 (2014).
- [121] A. N. Rudenko and M. I. Katsnelson, *Phys. Rev. B* **89**, 201408(R) (2014).
- [122] T. Deilmann and K. S. Thygesen, *2D Mater.* **5**, 041007 (2018).
- [123] J. Dai and X. C. Zeng, *Angew. Chem., Int. Ed. Engl.* **54**, 7572 (2015).
- [124] M. Van der Donck and F. M. Peeters, *Phys. Rev. B* **98**, 235401 (2018).
- [125] E. Cassette, R. D. Pensack, B. Mahler, and G. D. Scholes, *Nat. Commun.* **6**, 6086 (2015).
- [126] X. Wu, M. T. Trinh, and X.-Y. Zhu, *J. Phys. Chem. C* **119**, 14714 (2015).
- [127] F. Thouin, D. Cortecchia, A. Petrozza, A. R. Srimath Kandada, and C. Silva, *Phys. Rev. Research* **1**, 032032 (2019).
- [128] V. M. Axt and S. Mukamel, *Rev. Mod. Phys.* **70**, 145 (1998).
- [129] V. M. Agranovich, D. M. Basko, G. C. La Rocca, and F. Bassani, *J. Phys. Condens. Matter* **10**, 9369 (1998).
- [130] K. Abdel-Baki, F. Boitier, H. Diab, G. Lanty, K. Jemli, F. Lédée, D. Garrot, E. Deleporte, and J. Lauret, *J. Appl. Phys.* **119**, 064301 (2016).